A Comparison of the Bandelet, Wavelet and Contourlet Transforms for Image Denoising

Osslan Osiris Vergara Villegas[1], Humberto de Jesús Ochoa Domínguez[1] and Vianey Guadalupe Cruz Sánchez[2]
[1]*Universidad Autónoma de Ciudad Juárez (UACJ)*
Avenida del Charro No. 450 Norte Ciudad Juárez, Chihuahua, México
[2]*Centro Nacional de Investigación y Desarrollo Tecnológico (cenidet)*
Interior Internado Palmira S/N. Col. Palmira Cuernavaca, Morelos, México
{overgara, hochoa}@uacj.mx, vianey@cenidet.edu.mx

Abstract

The bandelet transform take advantage of the geometrical regularity of the structure of an image and is appropriate for the analysis of edges and textures of the images. Denoising is one of the most interesting and widely investigated topics in image processing area. The main problem in denosing is the tradeoff between the noise suppression and oversmoothing of image details. In order to solve that problem, in this paper we exploit the geometrical advantages offered by the bandelet transform to solve the problem of image denoising. We present the results obtained with the bandelet transform for denoising process with additive white Gaussian noise and salt and pepper noise. A comparison is made with those results obtained with wavelets and contourlets. We show that bandelets can outperform the wavelets and contourlets in terms of subjective and objective measures.

1. Introduction

A very important stage of any computer vision system is the image preprocessing. This step is performed in order to obtain better image quality, than the obtained at the acquisition stage.

In computer vision, we need to deal with a lot of data sets. Many scientific data sets are contaminated with noise, either because of the data acquisition process or because of naturally occurring phenomena [1]. Image denoising is the process of separating the noise out of the image, from a single observation of a degraded image.

Denoising is currently one of the most interesting and widely topics, investigated in image processing from both, a theoretical and an empirical point of view [2]. A common way to overcome the denoising difficulties is to remove the noise by using some techniques, to compute an approximation of the exact data that belongs to the proper function space [3].

The goal of image restoration is to relieve human observers from this task, by reconstructing a plausible estimate of the original image from the distorted or noisy observation. The problem of image denoising can be stated by equation 1 [2]:

$$g = f + n \tag{1}$$

Where g is the noisy signal, f is the clean signal and n the noise. The performance of the denoising method mainly depends on a suitable representation, able to compact as much as possible, the original information of the image in a few coefficients.

Denoising involves partitions of the data into the desirable components (signal) and undesirable components (noise). Separating the data into two parts requires milder assumptions than a complete analysis of all sources present. Validation is easier than those for more general techniques, and the tools require less expertise and pose less risk of misuse by inexperienced practitioners [3].

The classical techniques on image denoising are based on filtering [3]. However, new techniques based on the wavelet transforms [4], principal components analysis (PCA) [5] and independent component analysis (ICA) [6] have recently appear.

There are a lot of proposed algorithms that use wavelet transform to solve the image denoising problem [1], [2], [4]. Nevertheless, the wavelet denoising methods present some disadvantages when applied to natural images. To overcome this problem, new methods based on the contourlet transform have been proposed [7]. However, the image denoising

978-0-7695-3441-1/08 $25.00 © 2008 IEEE
DOI 10.1109/MICAI.2008.63

problem is still a great challenge. In this paper, we present the application of the bandelet transform to offer a novel solution to the image denoising problem. In the next sections we present the theory for denoising, the results obtained with bandelets and comparisons with contourlets and wavelets.

2. The Bandelet Transform

When natural images are processed, the geometrical structures inside become very important. Natural images are made of these structures which mostly are irregular or diffuse edges, high frequencies and several features that need very complicated methods to process. Therefore, it is important to know the geometrical structures of the images in order to exploit them. The geometry defines changing zones and gives important tracks for human perception.

There are several transforms that tackle the problem of image geometry such as the contourlet or bandelet transform. The second generation bandelet transform is a 2-D wavelet transform followed by a bandeletization. The bandelet is an orthogonal, multiscale transform able to preserve the geometric content of images and surfaces [8].

The orthogonal bandelets use an adaptive segmentation and a local geometric flow, which is well suited to capture the anisotropic regularity of edge structures. They are constructed with a "bandeletization" which is a local orthogonal transformation applied to wavelet coefficients [8].

The bandeletization removes the geometric redundancy of an image using an operator family. The operators can adapt the coefficients of a wavelet transform to the image geometry in order to capture the singularities of the image edges [9].

The bandelet transform use the image dyadic partition scheme, proposed for the x-lets. However, in each square, the geometry is not defined by localization; instead, it is defined by the orientation [10].

The orientation is defined by a vector field called geometric flow. The orientation is parallel to the discontinuities in every image point, and this generates a band. Each band is straightened into horizontal or vertical direction to put the geometric flow parallel to some shaft. The straighten operation is called warping.

The bandelet transform exploit the anisotropic regularity of natural images by constructing orthogonal vectors that are elongated in the direction where the function has a maximum of regularity [8].

3. Image Denoising with Bandelets

The simplest technique for image denoising is the thresholding method. In this method, we have as an input a noisy signal, and we perform a soft or hard thresholding scheme. The hard technique, sets to zero coefficients with values less than or equal to the threshold *T*. The soft technique, performs equal to the hard technique, but subtracts *T* from any coefficient that is greater than the threshold [11].

In the bandelet transform, a geometric flow of vectors is defined to represent the edges of an image. These vectors give the local directions in which the image has regular variations. Orthogonal bandelet bases are constructed by dividing the image support in regions which the geometric flow is parallel. In the bandelet basis $B(\Gamma) = \{b_v\}_v$, a thresholding algorithm defines an estimator f that can be computed with equation 2.

$$\tilde{f} = \sum_{v} S_T(\langle Y, b_v \rangle) b_v \tag{2}$$

Where Y is the noisy image, and the threshold is set to $T= \lambda\sigma$. Where σ is the noise variance, $\lambda = \sqrt{2\log_e(N)}$, and N is the number of pixels [8]. The function for thresholding is defined by equation 3.

$$S_T(x) = \begin{cases} x \ if \ |x| > T \\ 0 \ otherwise \end{cases} \tag{3}$$

The steps to compute the image denoising are:

1. Select an input square image.
2. Define the number of image partition squares (we select a value of 8 and we define none overlapping).
3. Compute the number of geometries in the image.
4. Perform a wavelet transform.
5. Compute the Lagrangian function (as a result we obtain the image geometries).
6. Compute the bandelet transform; we use a fixed segmentation tree.
7. Select the threshold (for this paper we select at least 3 noise levels).
8. Perform soft thresholding in the bandelet subbands.
9. Compute the inverse bandelet transform.

4. Tests and Results

In order to make the tests we use a set of 256 x 256 images with different frequency content. We classify the images in three groups: low, medium and high frequency groups. The images were classified by measuring their frequency content. In order to define this classification we transform the images into the wavelet domain using Daubechies db9 filter, and then we compute the energy of the wavelet coefficients in each subband using equation 4.

$$E_1 = \frac{1}{N^2} \sum_{k=1}^{N} \left| C_k \right|^2 \quad (4)$$

Where N is the image size and C_k is a wavelet domain coefficient. This classification measures the performance of images with different frequency content. The results of the classification is shown in table 1. The ranges were determined using [12] and are: medium frequency greater or equal than 95%, medium frequency from 99 to 99.49% and low frequency lower to 99%. The selected images are shown in figure 1.

The firs step is to add noise to the images using the equation 1. Then, we compute the standard deviation of the complete input image (f). The value obtained is divided by a parameter called *rho* which can take one values out of three. We use two different types of noise: Additive White Gaussian Noise (AWGN) and the Salt and Pepper Noise (SAPN) which are used to test denoising applications.

We compute the image threshold for each image in the wavelet, contourlet and bandelet domains. In figure 2, we show the recovered images after denoising with AWGN and = 0.01, the numerical results of the Peak signal to Noise Ratios (PSNRs) and the Signal to Noise Ratios (SNRs) are shown in table 2. The recovered images obtained with denoising from SAPN are shown in figure 3 and the numerical results in table 3.

Table 1. Numerical results of Image classification.

Classification	*Image*	*Wavelet Subband*			
		LL	*LH*	*HL*	*HH*
Low frequency	Apple	99.9697	0.0243	0.0041	0.0018
	Peppers	99.7610	0.1054	0.1151	0.0184
	Clown	99.7500	0.0775	0.1569	0.0157
	Goldhill	99.6635	0.1528	0.1587	0.0250
	Tomography	99.5456	0.2027	0.2311	0.0206
	Lena	99.5420	0.1080	0.2911	0.0588
Medium frequency	Barbara	99.3720	0.1685	0.3807	0.0789
	Lighthouse	99.3386	0.2590	0.3815	0.0209
	Star	99.2432	0.2637	0.2663	0.2267
	Oil filter	99.1432	0.3051	0.5021	0.0496
	Buthfish	99.0839	0.6491	0.8810	0.3859
	House	99.0748	0.3403	0.5597	0.0251
High frequency	Camman	98.9378	0.6033	0.3897	0.0692
	Baboon	98.9158	0.6017	0.2888	0.1937
	Satellite	98.7691	0.7717	0.4137	0.0454
	Nift7	98.3234	0.8943	0.6764	0.1058
	Letters	98.1810	0.5890	0.8155	0.4145
	Zone	80.2468	7.6932	7.6932	4.3669

Table 2. Numerical results obtained after image denoising with AWGN.

σ = 0.01	Noisy		Wavelet		Contourlet		Bandelet	
Image	**PSNR**	**SNR**	**PSNR**	**SNR**	**PSNR**	**SNR**	**PSNR**	**SNR**
Apple	75.63	10.21	76.65	11.22	82.60	17.18	75.45	10.03
Peppers	74.17	12.51	72.69	11.03	73.80	12.14	73.19	11.53
Clown	73.59	13.34	72.28	12.03	73.94	13.69	72.00	11.75
Goldhill	74.60	13.13	72.31	10.84	73.53	12.06	73.02	11.55
Tomography	72.60	11.96	72.24	11.61	75.04	14.41	71.80	11.17
Lena	74.23	12.31	73.26	11.33	74.92	12.99	73.09	11.16
Barbara	75.00	12.35	71.77	9.13	71.98	9.34	73.97	11.33
Lighthouse	74.14	11.61	73.07	10.54	75.03	12.50	73.60	11.07
Star	71.35	9.757	70.45	8.85	70.51	8.92	71.22	9.62
Oil filter	72.55	14.38	70.69	12.52	71.54	13.37	70.79	12.61
Buthfish	73.24	13.79	69.76	10.31	70.05	10.59	71.76	12.31
House	73.68	12.56	71.32	10.20	72.07	10.95	72.76	11.64
Camman	72.98	12.63	72.15	11.80	73.50	13.15	71.98	11.63
Baboon	75.95	11.61	72.12	7.78	72.12	7.78	74.94	10.60
Satellite	74.18	8.039	72.57	6.43	73.97	7.82	73.61	7.474
Nift7	72.53	13.65	69.40	10.51	69.46	10.57	71.18	12.29
Letters	71.69	12.38	70.35	11.03	68.35	9.03	71.69	12.37
Zone	72.32	15.15	66.82	9.66	66.71	9.55	71.11	13.95

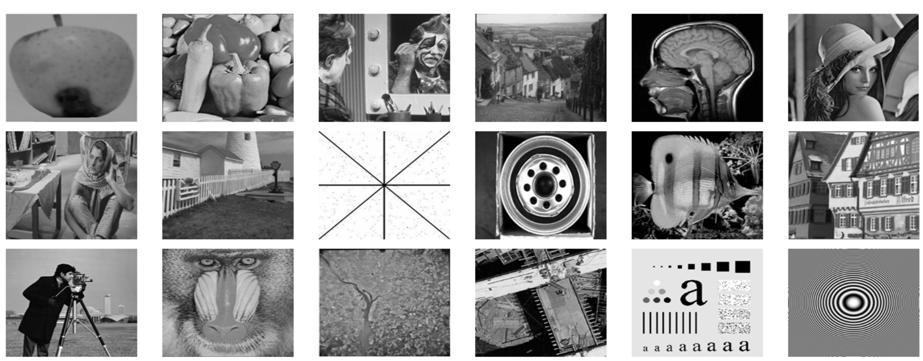

Fig. 1. Test images. First row: Apple, Peppers, Clown, Goldhill, Tomography, Lena. Second row: Barbara, Lighthouse, Star, Oil filter, Buthfish, House. Third row: Cameraman, Babbon, Satellite, Nift7, Letters, Zone.

Fig. 2. AWGN Denoised images. First column: Noisy images with AWGN and σ = 0.01. Second column: Denoised images using wavelets. Third column: Denoised images using contourlets. Fourth column: Denoised images using bandelets.

Fig. 3. SAPN denoised images. First column: Noisy images with AWGN and σ = 0.01. Second column: Denoised images using wavelets. Third column: Denoised images using contourlets. Fourth column: Denoised images using bandelets.

Table 3. Numerical results obtained after image denoising with SAPN.

σ = 0.01	Noisy		Wavelet		Contourlet		Bandelet	
Image	PSNR	SNR	PSNR	SNR	PSNR	SNR	PSNR	SNR
Apple	88.17	22.75	85.63	20.20	84.88	19.46	88.17	22.74
Peppers	88.13	26.47	75.15	13.49	74.10	12.44	79.79	18.13
Clown	88.09	27.84	74.82	14.57	74.23	13.98	76.88	16.64
Goldhill	88.11	26.64	74.14	12.67	73.76	12.29	77.49	16.02
Tomography	88.16	27.52	76.33	15.69	75.60	14.97	79.36	18.72
Lena	88.12	26.20	76.22	14.30	75.31	13.38	79.27	17.34
Barbara	88.14	25.50	73.24	10.59	72.17	9.52	80.33	17.69
Lighthouse	88.15	25.62	76.02	13.49	75.60	13.07	82.51	19.97
Star	88.12	26.52	75.22	13.62	71.11	9.52	85.69	24.10
Oil filter	88.13	29.96	72.41	14.24	71.84	13.67	75.24	17.07
Buthfish	88.09	28.64	71.02	11.57	70.18	10.73	76.78	17.33
House	88.12	27.00	73.14	12.02	72.40	11.28	79.38	18.26
Camman	88.11	27.76	74.92	14.57	73.79	13.44	78.56	18.21
Baboon	88.14	23.79	73.50	9.16	72.36	8.01	80.99	16.65
Satellite	88.13	21.99	76.05	9.91	75.01	8.87	82.08	15.94
Nift7	88.19	29.30	70.69	11.81	69.70	10.81	76.47	17.59
Letters	88.14	28.83	73.77	14.46	68.71	9.40	89.46	30.15
Zone	88.14	30.97	67.58	10.42	66.99	9.82	76.64	19.48

4.1. Discussion

We measure the PSNR and the SNR because they are typical measures widely used for denoising. All the transforms performs better when AWGN is present, this can be probed with the numerical results.

The performance of the denoising algorithm using bandelet performs well even when we have an image with very high frequencies. It is important preserve the details in order to avoid oversmoothing them. The higher the noise variance the worse the performance of the algorithm however, the edges of the images are preserved.

The objective measures are not always a good parameter to measure the quality of the denoised image. Therefore, we perform subjective tests asking some people their opinion of each recovered image. The images with best qualification were always those processed with the bandelet transform.

In figure 4 we show the bandelet SNR plot with different noise variances for three different images pertaining to one of the three groups.

Image cleaning is more difficult when SAPN is present. In both types of noise, the results of the measurements are low. However, if we made a visually test we can see the edges better preserved with the bandelet transform.

With the results obtained we can conclude that bandelet transform is a good tool for image denoising even when we have very high frequency images as input.

In figure 5 we show a close up of the Barbara image. The wavelet and the contourlet miss a part of the elbow while the bandelet preserve this part of the image after the denoising process.

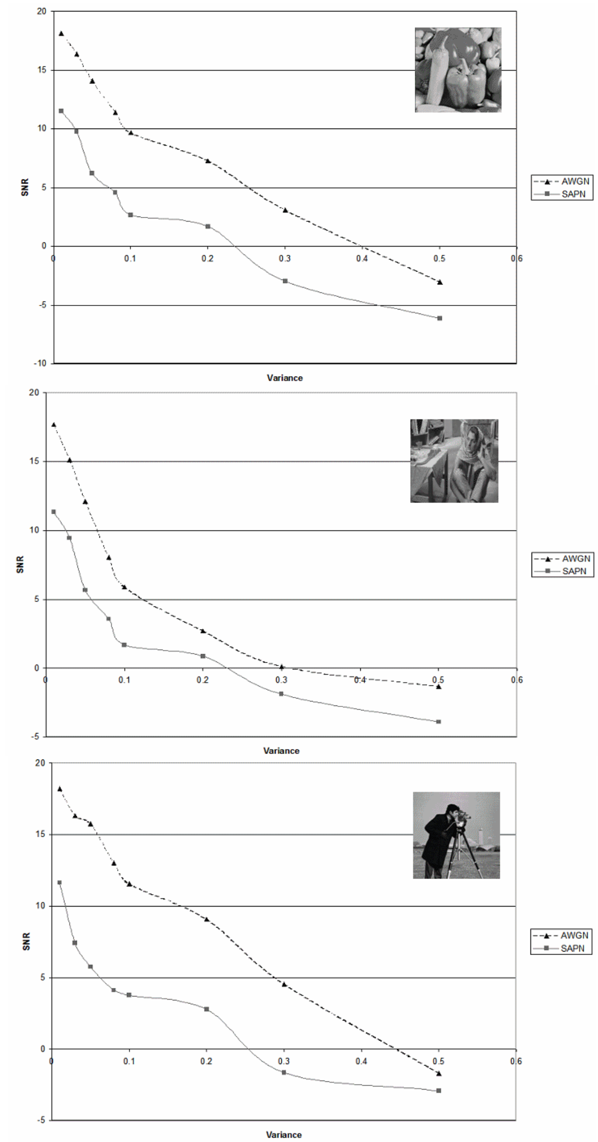

Fig. 4. Bandelet SNR plots for Peppers, Barbara and Cameraman.

5. Conclusions and Further Works

Image denoising is still an open problem in digital image processing. Several algorithms have been proposed in the literature. In this paper we presented a comparison of three novel methods applied to denoising and presented a new denoising algorithm using the bandelet transform. The algorithm performs very well even with images of high frequency content, because it can tackle the classic problem of image oversmoothing and edge preservation.

The comparison presented with three transforms allows us to check the superiority of the bandelet transform over the wavelet and contourlet. We need to design an intelligent system to select the better threshold for each image according to its frequency content.

In the future we are going to work into defining a strategy to exploit the bandelet transform for image compression, we are planning to design a coder that allow us to preserve the important features of the images such as textures, edges and edge associated details.

Fig. 5. Close up of the denoised Barbara elbow. The upper left corner is the noisy image, the upper right corner is the result obtained with wavelets, the lower left corner the result obtained with contourlets and the lower right corner the result obtained with bandelets.

6. References

[1] K. Q. Huanga, Z. Y. Wub, S. K. Fungc and H. Y. Chan, “Color Image Denoising with Wavelet Thresholding Based on Human Visual System Model”, *Signal Processing: Image Communication*, vol. 20, no. 2, February 2005, pp. 115 – 127.

[2] V. Bruni and D. Vitulano D., “Combined Image Compression and Denoising Using Wavelets”, *Signal Processing: Image Communication*, vol. 22, no. 1, January 2007, pp. 86 – 101.

[3] A. Cheveigné and J. Simon, “Denoising Based on Spatial Filtering”, *Journal of Neuroscience Methods*, vol. 171, no. 2, June 2008, pp. 331 – 339.

[4] D. Lazzaro and L. Montefusco, “Edge-Preserving Wavelet Thresholding for Image Denoising”, *Journal of Computational and Applied Mathematics*, vol. 210, no. 1-2, December 2007, pp. 222 – 231.

[5] S. Bacchelli and S. Papi, “Image Denoising Using Principal Component Analysis in the Wavelet Domain”, *Journal of Computational and Applied Mathematics*, vol. 189, no. 1, May 2006, pp. 606 – 621.

[6] A. Hyvärinen and E. Oja, “Independent Component Analysis: Algorithms and Applications”, *Neural Networks*, vol 13. no. 4-5, May-June 2000, pp.411 -430.

[7] A. L. da Cunha, J. Zhou and M. N. Do, “The Nonsubsampled Contourlet Transform: Theory, Design, and Applications”, *IEEE Transactions on Image Processing*, vol. 15, no. 10, October 2006, pp. 3089 – 3101.

[8] S. Mallat and G. Peyré, “A Review of Bandlet Methods for Geometrical Image Representation”, *Numerical Algorithms*, vol. 44, no. 3, March 2007, pp. 205 – 234.

[9] S. Mallat and E. LePennec, “Sparse Geometric Image Representation with Bandelets”, *IEEE Transaction on Image Processing*, vol 14, no. 4, April 2005, pp. 423-438.

[10] M. N. Do and M. Vetterli, “The Contourlet Transform: An Efficient Directional Multiresolution Image Representation”, *IEEE Transactions on Image Processing*, vol. 14, no. 12, December 2005, pp. 2091 – 2106.

[11] D. L. Donoho, “De-noising by Soft-Thresholding”, *IEEE Transactions on Information Theory*, vol. 41, no 3. May 1995, pp. 613-627.

[12] H. J. Barnard, Image and Video Coding Using a Wavelet Decomposition, Ph. D. Dissertation, Delft Technological University, Electrical Engineering Department, The Netherlands, 1994.